Environmental Research Letters

LETTER • OPEN ACCESS

Spatiotemporal patterns of rain-on-snow and basal ice in high Arctic Svalbard: detection of a climate-cryosphere regime shift

To cite this article: Bart Peeters *et al* 2019 *Environ. Res. Lett.* **14** 015002

Environmental Research Letters

CrossMark

OPEN ACCESS

RECEIVED
19 June 2018

REVISED
6 November 2018

ACCEPTED FOR PUBLICATION
9 November 2018

PUBLISHED
8 January 2019

LETTER

Spatiotemporal patterns of rain-on-snow and basal ice in high Arctic Svalbard: detection of a climate-cryosphere regime shift

Bart Peeters[1,7], **Åshild Ønvik Pedersen**[2], **Leif Egil Loe**[3], **Ketil Isaksen**[4], **Vebjørn Veiberg**[5], **Audun Stien**[6], **Jack Kohler**[2], **Jean-Charles Gallet**[2], **Ronny Aanes**[1,2] **and Brage Bremset Hansen**[1]

[1] Centre for Biodiversity Dynamics, Department of Biology, Norwegian University of Science and Technology, NO-7491 Trondheim, Norway
[2] Norwegian Polar Institute, Fram Centre, NO-9296 Tromsø, Norway
[3] Norwegian University of Life Sciences, Department of Ecology and Natural Resource Management, PO Box 5003, NO-1432 Ås, Norway
[4] Norwegian Meteorological Institute, PO Box 43, Blindern, NO-0313 Oslo, Norway
[5] Norwegian Institute for Nature Research, PO Box 5685, Torgarden, NO-7485 Trondheim, Norway
[6] Norwegian Institute for Nature Research, Fram Centre, NO-9296 Tromsø, Norway
[7] Author to whom any correspondence should be addressed.

E-mail: bart.peeters@ntnu.no

Keywords: climate change, ground ice, rain-on-snow, snowpack, synchrony, topography, meteorology

Supplementary material for this article is available online

Abstract

Arctic winters have become increasingly warmer and rainier. Where permafrost prevails, winter rain (or rain-on-snow) is known to occasionally cause extensive ice layers at the snow/ground interface, i.e. 'basal ice' or 'ground ice', with potentially large ecological and socio-economic implications. However, an overall lack of field data has so far restricted our predictive understanding of the environmental conditions shaping spatiotemporal variation in basal ice. Here, we use time-series of spatially replicated snowpack measurements from coastal (Ny-Ålesund area; 2000–2017) and central Spitsbergen (Nordenskiöld Land; 2010–2017), Svalbard, to analyze spatiotemporal patterns in basal ice and how they are linked with topography, weather, snowpack and climate change. As expected, both the spatial occurrence and thickness of basal ice increased strongly with the annual amount of winter rain. This effect was modified by accumulated snowfall; a deeper snowpack restricts ice formation following a minor rain event, but enhances ice formation following heavy rain due to an increased contribution of snowmelt. Accordingly, inter-annual variation in snow depth was negatively related to basal ice thickness. Annual fluctuations in basal ice thickness were strongly correlated in space (average correlation $\rho = 0.40$; 0–142 km distance between plots) due to strong spatial correlation in winter rain ($\rho = 0.62$; 14–410 km distance between meteorological stations). Models of basal ice based on meteorological time-series (1957–2017) suggested that ice-free winters (i.e. mean basal ice <0.1 cm) had virtually not occurred since 1998, whereas such winters previously (1957–1998) occurred every three–four years on average. This detected cryosphere regime shift was linked to a parallel climate regime shift with increased winter rain amounts. Svalbard is regarded a bellwether for Arctic winter climate change. Our empirical study may therefore provide an early warning of future changes in high-arctic snowpacks.

Introduction

In the Arctic, winter warm spells with near-surface air temperatures above 0 °C are becoming more frequent due to global warming (Moore 2016, Graham *et al* 2017). This warming, in combination with enhanced surface evaporation due to the loss of sea-ice cover and poleward atmospheric moisture transport, contributes to an overall increase in precipitation over Arctic land areas (4.5% increase per degree of temperature rise), particularly in late autumn and winter (Serreze *et al* 2009, Zhang *et al* 2012, Bintanja and Selten 2014). Recent climate models indicate that rainfall will likely become the dominant form of winter precipitation

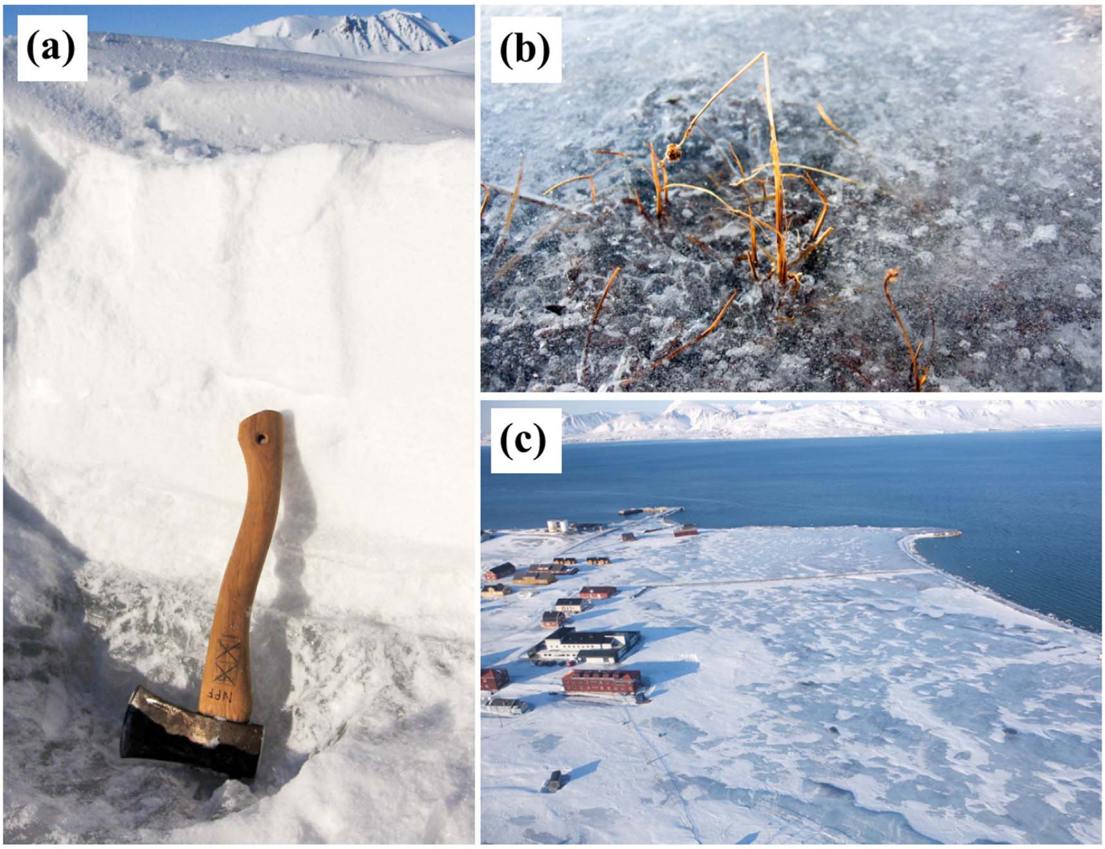

Figure 1. (a) Snow profile from a vegetated tundra site near Ny-Ålesund, Svalbard, showing a thick ice layer ('basal ice') at the bottom of the snowpack. (b) Because of the short-growing vegetation at such high latitudes, basal ice may encapsulate most of the plants. (c) In some winters, basal ice covers most of the tundra at low altitudes, such as the surroundings of Ny-Ålesund.

during the 21st century (Rennert *et al* 2009, Bintanja and Andry 2017). The rain-on-snow (ROS) phenomenon (Putkonen and Roe 2003) is of particular concern as it can lead to avalanches (Conway and Raymond 1993), increased ground surface temperature and near-surface permafrost thawing (Isaksen *et al* 2007, Westermann *et al* 2011), and ice-wedge cracking if water freezes after infiltrating the soil (Christiansen *et al* 2013). Furthermore, heavy ROS events can lead to thick ice layers within the snowpack or at the snow/ground interface, i.e. 'basal ice' or 'ground ice', across the landscape (figure 1; e.g. Vikhamar-Schuler *et al* 2013).

Several studies have documented negative effects of ROS and basal ice on small and large herbivores (Kausrud *et al* 2008, Stien *et al* 2012), soil invertebrates (Coulson *et al* 2000), vegetation growth and reproduction (Bjerke 2011, Preece *et al* 2012, Milner *et al* 2016, Bjerke *et al* 2017), and even whole vertebrate communities (Hansen *et al* 2013). The most noticeable consequences are the occasional die-offs of Arctic ungulates due to mass starvation, as the impenetrable layer of ice makes vegetation inaccessible (e.g. Parker *et al* 1975, Forchhammer and Boertmann 1993, Miller and Gunn 2003, Kohler and Aanes 2004, Hansen *et al* 2011, Langlois *et al* 2017). More frequent ROS and basal ice formation in space and time may therefore also have serious socio-economic impacts for reindeer herders (Bartsch *et al* 2010, Forbes *et al* 2016, Riseth *et al* 2016), but also for the tourism industry and local communities in the Arctic (Hansen *et al* 2014).

Basal ice is formed when liquid water, deriving from snowmelt and/or rainfall (ROS), pools at the bottom of the snowpack and freezes as latent heat is transferred to the surrounding snowpack and frozen ground (Woo *et al* 1982, Putkonen and Roe 2003, Westermann *et al* 2011). In winter, small amounts of rainfall or melted snow resulting from solar radiation and warm air temperatures (Hock 1999) can be absorbed within the snowpack, where it freezes along lateral flow channels (Marsh and Woo 1984). However, as the snowpack becomes saturated, sufficient amounts of rainfall can percolate vertically through the snowpack and freeze in contact with the frozen ground (Woo *et al* 1982, Marsh and Woo 1984, Conway and Benedict 1994). During ROS events, a considerable proportion of total snowpack runoff can be caused by snowmelt (27% on average in the Swiss Alps, Würzer *et al* 2016). Heat fluxes from warm, moist, and windy conditions can be responsible for the main snowmelt energy input (e.g. Marks *et al* 1998). However, advective heat from rain is a potentially large additional source for melt energy (Würzer *et al* 2016). This is particularly the case in the Arctic, where shortwave radiation is not available for melting during the polar night, and near-surface air temperatures need to be several degrees above freezing point to sufficiently increase snowmelt rates (Hock 1999, Putkonen and Roe 2003). Accordingly, in high-arctic environments where permafrost prevails, the formation of basal ice layers is typically associated with heavy ROS and concurrent snowmelt during warm spells (Putkonen and Roe 2003, Kohler and Aanes 2004, Bartsch *et al* 2010, Vikhamar-Schuler *et al* 2013, Hansen *et al* 2014).

Because of a general lack of field data time-series from the high Arctic (but see Kohler and Aanes 2004, Hansen *et al* 2011 for Svalbard, and Bulygina *et al* 2010, for Northern Eurasia), our empirical understanding of the spatial and temporal variation in basal ice occurrence remains poor. Some studies have used proxies or simulations based on meteorological or satellite data (e.g. Grenfell and Putkonen 2008, Bartsch *et al* 2010, Vikhamar-Schuler *et al* 2013, Langlois *et al* 2017), without validation from *in situ* field data. Furthermore, little is known on the spatial extent of basal ice events and how they are linked to large-scale meteorological patterns (but see Bartsch *et al* 2010, Forbes *et al* 2016).

In this study, we address this by taking advantage of time-series of spatially replicated snow and basal ice measurements from coastal (Ny-Ålesund area; 2000–2017) and central Spitsbergen (Nordenskiöld Land, near Longyearbyen; 2010–2017), Svalbard, combined with data from local meteorological stations. First, we investigated combined effects of topography, temperature and precipitation patterns, and climate change on basal ice occurrence and thickness. To make our approach applicable across study areas and scientific disciplines, we built simple regression models based on commonly available data from meteorological stations and topographic information from digital elevation models. We then investigated how the spatial extent of basal ice events across our study area was linked to spatial correlation in winter rain. Finally, we modelled and predicted historical occurrence and thickness in basal ice using our regression models accounting for weather and topography, and investigated temporal changes linked with the recent warming in high Arctic Svalbard (Hansen *et al* 2014, Isaksen *et al* 2016).

Materials and methods

Study area

The two study areas are located in coastal and central Spitsbergen, Svalbard (74–81 °N, 10–35 °E; figure 2(a)). The coastal study area in North–West Spitsbergen, hereafter referred to as 'NW coast', consists of the mountainous peninsula Brøggerhalvøya, where the research settlement Ny-Ålesund is located, and the two peninsulas Sarsøyra and Kaffiøyra, which are characterized by flat coastal planes with steep mountains to the East (figure 2(b)). The study area in Central Spitsbergen is located 17–33 km south of the meteorological station at Svalbard Airport, Longyearbyen, and covers the valleys Colesdalen, Semmeldalen and Reindalen (figure 2(c)). The climate in these parts of the Svalbard archipelago, and particularly the NW coast, is influenced by the North-Atlantic current and the coupled sea-ice-ocean atmosphere system (Benestad *et al* 2002). Annual total precipitation and mean temperature for 1970–2015 were on average 417 mm and −5.1 °C for Ny-Ålesund, and 194 mm and −5.0 °C for Svalbard Airport.

In our study, winter was defined as the period between 1 November (preceding year) and 31 March, i.e. just prior to the basal ice measurements. The main reason for the 1 November cut-off is that the onset of ground surface freezing, although depending on the landform, generally occurs some time during October (Eckerstorfer *et al* 2017). In addition, during the study period (2000–2017), daily air temperatures were often <0 °C in November (mean ± SD = −6.5 ± 5.3 °C for Svalbard Airport and Ny-Ålesund combined), and less so in October (−3.2 ± 4.4 °C). Total winter precipitation and mean winter temperature were on average 204 mm and −11.2 °C in Ny-Ålesund, and 88 mm and −11.8 °C at Svalbard Airport. However, a strong winter warming has been identified during the last decades (Førland *et al* 2011), and warm spells with above-zero temperatures now occur more frequently (Hansen *et al* 2014, Vikhamar-Schuler *et al* 2016).

Climate-cryosphere data

Snow profiles and basal ice were sampled in April/early May (earliest 29 March, latest 9 May). Snow pits were dug manually using a spade and, if basal ice was present, an axe or drill was used to reach the ground surface (figure 1(a)). Snow depth, basal ice thickness and the total thickness of ice layers within the snowpack were measured. Data were collected for a total of $n = 2\ 539$ observations during the period 2010–2017 in Central Spitsbergen and 2000–2017 (except 2001 and 2009) in NW coast (figures 2(b)–(c), 3(a)–(b); see supplementary material 1, available online at stacks.iop.org/ERL/14/015002/mmedia). In Central Spitsbergen, sampling was conducted annually at the same sites ($n = 128$), which were spatially structured at eight different locations following a hierarchical block design (see Loe *et al* 2016). Plots at each location covered ridges and sub-ridges at the smallest scale (5 m apart), and valley bottoms and flat hilltops at the largest scale (500 m apart). On the NW coast, snow-ice data were combined from three studies with varying sampling design (see supplementary material 1 for details). These included both randomly placed snow pits along transect lines (2000, 2002–2007, 2010, 2012–2015; Kohler and Aanes 2004) and repeated measures at fixed sites following either a randomly placed grid system (2005–2012, except 2009; Hansen *et al* 2011) or a similar hierarchical block

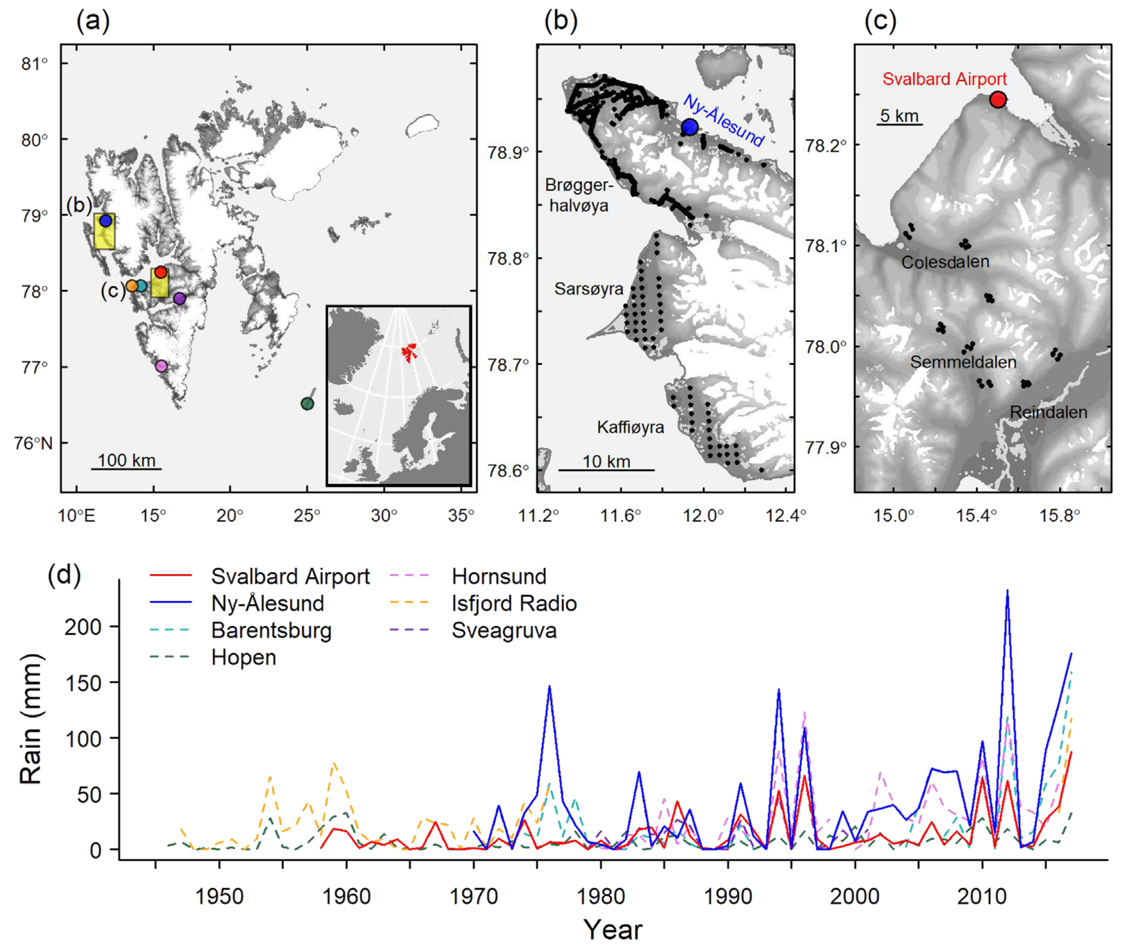

Figure 2. (a) Map of Svalbard (in red in the inset map), situated in the Arctic Ocean north of Norway. Coloured circles indicate the location of the seven meteorological stations used in this study. Yellow rectangles indicate study areas on (b) the NW coast near the meteorological station at Ny-Ålesund and in (c) Central Spitsbergen near the station at Svalbard Airport, Longyearbyen. Black dots in (b)–(c) indicate sample plot locations for cryosphere measurements. (d) Time-series of winter rain (November–March) for the seven meteorological stations across Svalbard.

design as in Central Spitsbergen (2013–2017; this study).

Daily average air temperature and amount of precipitation were obtained for seven meteorological stations across Svalbard (figure 2(a); table S1.2). All stations were used to analyze spatiotemporal patterns of winter rain, while only the meteorological stations in Ny-Ålesund and at Svalbard Airport were used for the basal ice analyses of the NW coast and Central Spitsbergen study areas, respectively. Winter (November–March) precipitation was classified as rain when daily average temperature $\geqslant$1 °C (Stien *et al* 2012, Hansen *et al* 2013). Note that a large rain event (R. Aanes pers. obs.) occurred on 24 March 2007 in Ny-Ålesund (67.3 mm), however with air temperatures ranging from −3.3 °C to 3.8 °C (mean = −0.3 °C), which was included when calculating the variable Rain, i.e. total amount of winter rain (mm; figures 2(d), 3(c)). The 'peak rain event' for each winter was defined as the largest rainfall over a three-day period. Daily precipitation classified as snow (i.e. at temperatures <1 °C) was then summarized from 1 November until this event to obtain the variable Snow_P, i.e. the accumulated amount of snowfall until the peak rain event (mm; figure 3(d)). Winter heat sum was calculated by accumulating daily temperatures >0 °C for November–March (figure 3(e)).

Data analysis

First, we compared annual basal ice occurrence (presence/absence, where presence $\geqslant$ 0.5 cm basal ice) and thickness (cm on natural logarithmic (hereafter log) scale) between the NW coast and Central Spitsbergen for the period in which the time-series overlap (2010–2017). We also investigated how average snow depth measured in late winter (April/early May) was related to average observed basal ice thickness, accounting for accumulated snowfall (November–March), in the two study areas (see supplementary material 2 for details on the data analysis).

Second, we used mixed-effects regression models to investigate the effects of climate and topography on the occurrence and thickness of basal ice. One major advantage of mixed models is that they can account for temporal and spatial autocorrelation as well as

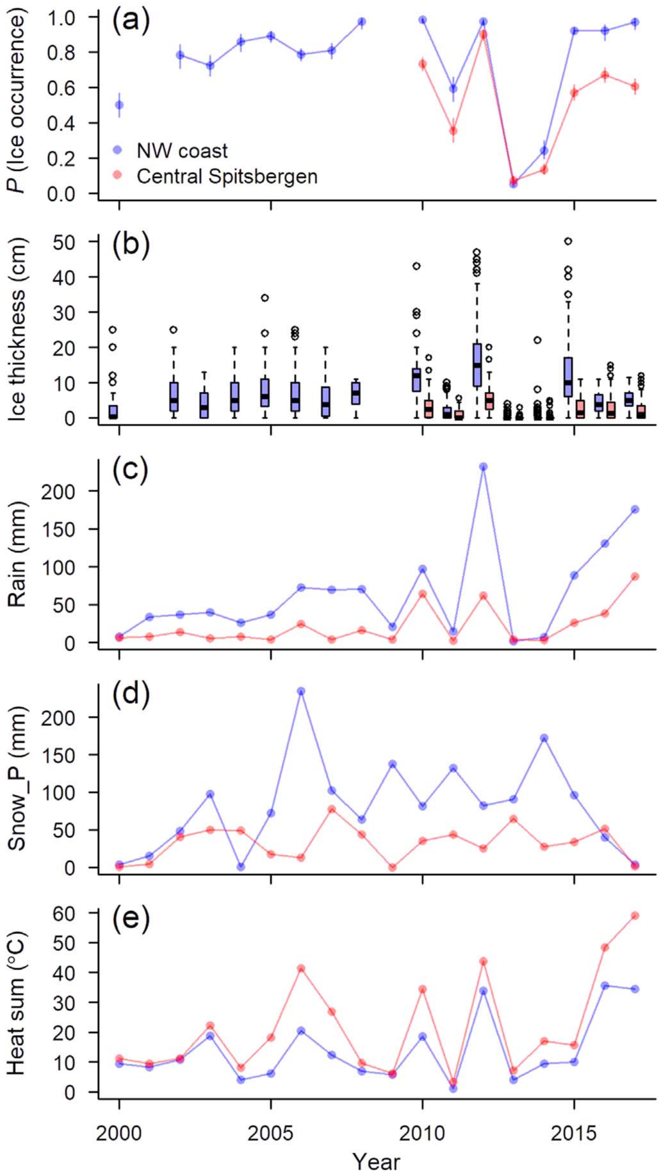

Figure 3. Time-series of data used in the basal ice analyses. (a) Basal ice occurrence, i.e. proportion of sampling sites with basal ice presence (mean ± SE). (b) Basal ice thickness (boxplots showing the median, 1st and 3rd quartile (box), with whiskers and dots indicating 1.5 times the interquartile range and outliers, respectively). (c) Amount of winter rain (November–March). (d) Accumulated amount of snowfall from 1 November until the peak rain event (Snow_P). (e) Winter heat sum, i.e. accumulated temperature above 0 °C (November–March). Basal ice data from the NW coast (2000, 2002–2008, 2010–2017) and Central Spitsbergen (2010–2017), and weather data from their local stations in Ny-Ålesund and at Svalbard Airport, are shown in blue and red, respectively.

unbalanced repeated observations (Cnaan *et al* 1997). *A priori*, we expected to find a positive effect of winter rain on ice occurrence and thickness (Putkonen and Roe, 2003), possibly modified by the amount of accumulated snowfall (Würzer *et al* 2016). We also tested for an effect of total accumulated heat sum as snowpack warming may lead to snow melting and refreezing at the bottom of the snowpack. Elevation (m a.s.l.) and Slope (degrees) at the sample plot level, derived from a Digital Elevation Model with a 20 m resolution (http://geodata.npolar.no), were included to account for topographic effects on basal ice. To evaluate the best fitting parameters, we performed model selection over candidate models using Akaike's information criterion (Burnham and Anderson 2002; see supplementary material 2 and 4).

Third, to quantify the spatial scales at which winter rain and basal ice occur, we analyzed spatial correlation in annual fluctuations of winter rain and ice thickness between pairs of meteorological stations or sampling sites, respectively. For this, we implemented a nonparametric covariance function on pairwise correlations (ρ) as a function of distance (Bjørnstad and Falck, 2001). To investigate the contribution of rain to the spatial correlation in basal ice, we first fitted log-linear models of basal ice thickness with rain as a predictor for every sampling site, and then analyzed the spatial correlation in annual fluctuations of the

Table 1. Parameter estimates (β) with standard errors (SE) of standardized fixed effects covariates from the generalized linear mixed model (GLMM) and linear mixed model (LMM) of basal ice occurrence (on logit scale) and thickness, respectively. Rain, Snow_P (i.e. accumulated snowfall until the peak rain event) and Ice thickness were log-transformed in the analysis. Standard deviations (SD) and number of groups (n) are given for random effects on the intercept. Marginal and conditional R^2 indicate variance explained by the fixed effects and by both fixed and random effects, respectively (Nakagawa and Schielzeth 2013).

	Ice occurrence (GLMM)		Ice thickness (LMM)	
Fixed effects	$\beta \pm SE$	*P*-value	$\beta \pm SE$	*P*-value
Intercept	0.904 ± 0.197	<0.001	1.180 ± 0.100	<0.001
Elevation	-0.527 ± 0.085	<0.001	-0.214 ± 0.024	<0.001
Slope	-0.162 ± 0.082	0.048	-0.142 ± 0.024	<0.001
Rain	1.675 ± 0.160	<0.001	0.493 ± 0.059	<0.001
Snow_P	-0.159 ± 0.109	0.143	0.034 ± 0.052	0.648
Rain : Snow_P	0.361 ± 0.129	0.005	0.227 ± 0.044	<0.001
Rain : elevation	—	—	-0.106 ± 0.017	<0.001
Random effects	SD	*n*	SD	*n*
Year	0.482	16	0.322	16
Location	0.441	13	0.175	13
Plot ID	0.339	1,282	0.239	1,282
R^2	Marginal	Conditional	Marginal	Conditional
	0.496	0.567	0.436	0.601

residuals from these models (see supplementary material 2 for details).

Finally, we investigated temporal changes in winter rain and basal ice. For this, we modelled and predicted past basal ice occurrence and thickness by using historical weather data (since 1958 and 1970 for Svalbard Airport and Ny-Ålesund, respectively) applied to our top-ranked regression models (supplementary material 4). Preliminary analyses suggested that changes over time were clearly not following linear trends. Thus, we tested for regime shifts (i.e. inter-decadal fluctuations in average levels; Overland *et al* 2006) in the time-series of winter rain and modelled basal ice (supplementary material 2).

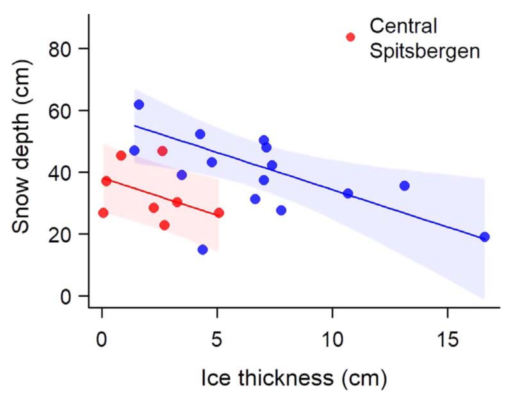

Figure 4. Relationship between average snow depth and basal ice thickness, measured at the same time in April, in the NW coast ($n = 16$ years; blue) and Central Spitsbergen ($n = 8$; red) study areas. Regression lines are shown with 95% CI (shaded areas; see table S3 for parameter estimates).

Results

The average amount of winter rain (mm; log scale) was more than twice higher on the NW coast than in Central Spitsbergen (paired t-test: $t = 4.27$, d.f. $= 47$, $P < 0.001$). Similarly, average basal ice thickness (cm; log scale) on the NW coast was on average twice the estimate for Central Spitsbergen (estimated ratio $= 2.0 \pm 0.7$; figure 3(b)), while the spatial occurrence of basal ice was also more extensive during most winters (figure 3(a)). Furthermore, late winter snow depth (measured in April/early May) was on average 53% deeper on the NW coast, and was more shallow in years with thick basal ice layers, independent of snowfall amount (figure 4, table S3).

Annual fluctuations in basal ice occurrence and thickness largely followed the fluctuations in winter rain (figure 3). Accordingly, the model selection for the regression analyses (supplementary material 4) indicated that the amount of winter rain was the strongest predictor of basal ice, with a positive effect on both occurrence and thickness (table 1, figure 5). As expected, there was a positive interaction between rain and accumulated snowfall (Snow_P) due to melting and refreezing processes in the snowpack (e.g. Woo *et al* 1982, Würzer *et al* 2016). Large amounts of snowfall (high Snow_P, i.e. presumably deep snow accumulation) prevented the formation of basal ice when there was only minor rainfall, but resulted in thicker basal ice when associated with major rain events. Accordingly, shallow late-winter snow depths recorded in years with particularly icy conditions (figure 4) were likely associated with more rain-induced snowmelt. At

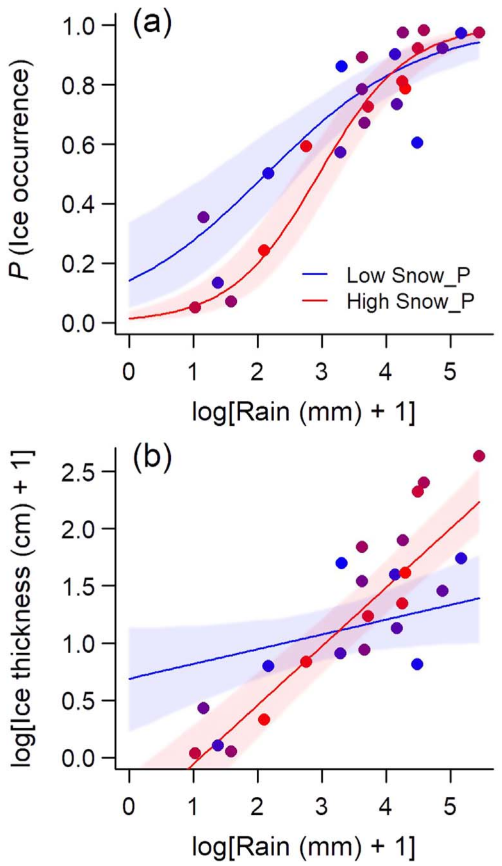

Figure 5. Annual variation in basal ice is explained by the interaction between winter rain and snow. Estimated effects (regression slopes) of winter rain (log scale) are shown for basal ice (a) occurrence (probability) and (b) thickness (log scale), and at low (blue; mean − 1SD) versus high (red; mean + 1SD) amounts of accumulated snowfall until the peak rain event (Snow_P). Shaded areas indicate 95% CI from 1000 parametric bootstrap iterations. Observed means (one dot per year and study area) follow a colour gradient from low (blue) to high (red) amounts of Snow_P.

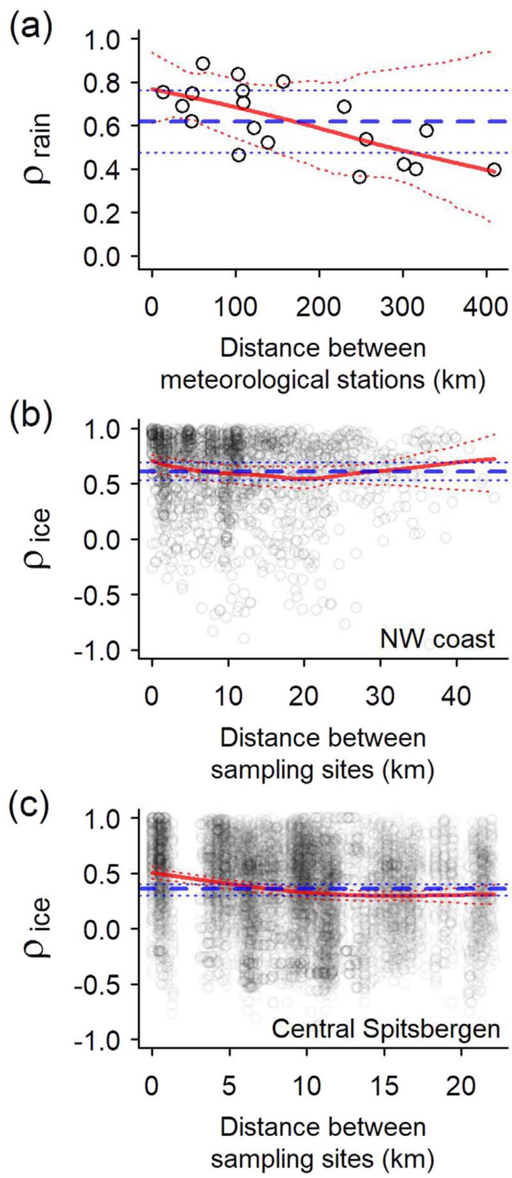

Figure 6. Spatial correlation in annual fluctuations of winter rain and basal ice thickness. (a) Correlation (ρ) in annual fluctuations of winter rain between meteorological stations across Svalbard ($n = 19$ pairwise correlations (circles) with at least five years overlap in time-series). (b)–(c) Correlation in basal ice thickness between sampling sites in (b) the NW coast study area ($n = 1\,676$ pairwise correlations) and (c) Central Spitsbergen ($n = 8\,035$ pairwise correlations). The average spatial, i.e. 'regional', correlation (dashed blue line) and nonparametric covariance of pairwise correlations as a function of distance (solid red line) are shown with 95% CI (dotted lines).

the local scale, basal ice occurrence and thickness decreased with higher elevation and steeper slopes (table 1). Furthermore, the positive effect of rain on basal ice thickness decreased with increasing elevation, because precipitation is more likely to fall as snow at higher altitudes.

Annual fluctuations in winter rain were strongly correlated over distances up to 410 km (i.e. the max distance between meteorological stations), with an average spatial or 'regional' correlation of $\rho = 0.62$ [95% CI: 0.48, 0.76] (figure 6(a)). However, the spatial correlation in winter rain gradually decreased with distance between the meteorological stations. Similarly, annual measurements of basal ice thickness were strongly correlated between sampling sites within and between the two study areas. The regional correlation in basal ice thickness was higher on the NW coast ($\rho = 0.61$ [95% CI: 0.53, 0.68]) than in Central Spitsbergen ($\rho = 0.36$ [95% CI: 0.31, 0.41]; figures 6(b)–(c)), but remained high across the two study areas ($\rho = 0.40$ [95% CI: 0.36, 0.45]; figure S6(a)). After accounting for the effect of rain, the regional correlation in basal ice thickness (i.e. the correlation in model residuals) was close to zero ($\rho = 0.06$ [95% CI: 0.02, 0.10]; figure S6(b)). Accordingly, and as expected, the strong spatial correlation in temporal variation of basal ice thickness across the landscape and study areas was mainly due to the strong spatial correlation in winter rainfall.

Historical weather data from Svalbard Airport and Ny-Ålesund (continuous time-series available since 1957 and 1969, respectively) indicated that winters with virtually no rain occurred approximately every third to fourth year until 1998 (figures 7(a)–(b)). Based

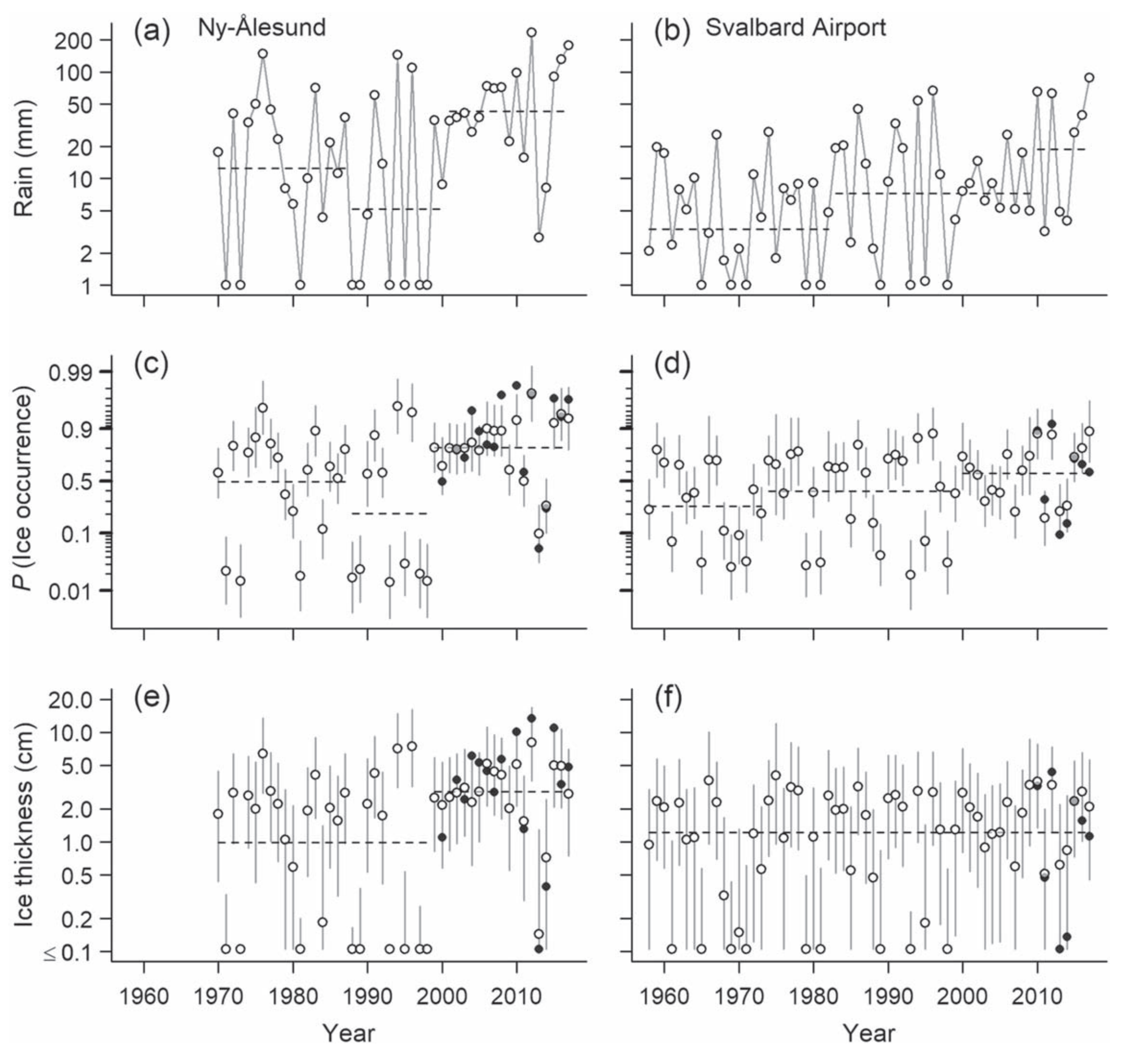

Figure 7. Regime shifts in (a)–(b) historical amount of winter rain (*y*-axis on log scale), and past modelled basal ice (c)–(d) occurrence (probability on logit scale) and (e)–(f) thickness (*y*-axis on log scale), for the meteorological stations in (a), (c), (e) Ny-Ålesund, NW coast, and at (b), (d), (f) Svalbard Airport, Central Spitsbergen. Estimated basal ice occurrence and thickness are shown for slope of 6° (i.e. average slope in sampling sites) at 50 m elevation (white dots; error bars show 95% prediction intervals). Average observed values up to 200 m elevation are indicated with black dots (or grey when overlapping with model estimates). Horizontal dashed lines indicate average values before and after observed change points, i.e. regime shifts ((a) 1987, 2000; (b) 1982, 2009; (c) 1987, 1998; (d) 1973, 1999; (e) 1998; (f) no change point observed).

on change point analyses, we detected a climate regime shift with an overall increase in the average amount of winter rain (log scale) around the turn of the century. Accordingly, when our best-ranked mixed-effects models were used to model basal ice occurrence and thickness based on historical weather data, we also detected a climate-related regime shift in the frequency of icy winters (figures 7(c)–(f)). Rain- and ice-free winters have virtually not occurred since 1998. On the NW coast (Ny-Ålesund), the modelled occurrence of basal ice in the landscape (at an arbitrary elevation of 50 m a.s.l.) was on average 49% before 1987, 20% between 1987 and 1998, and 80% after 1998 (figure 7(c)). Modelled average basal ice thickness increased almost three-fold from 0.99 to 2.88 cm before and after 1998, respectively (figure 7(e)). Also, for Central Spitsbergen (Svalbard Airport), a recent change point in the time-series of modelled basal ice occurrence was detected in 1999, when average ice occurrence increased from 40% to 58% before and after, respectively (figure 7(d)). Here, no change point was detected for ice thickness, but winters with very low ice thickness have been virtually absent since 1998 (figure 7(f)).

Discussion

In the present study, we used spatiotemporal modelling of long-term field data from the high Arctic archipelago of Svalbard to demonstrate the occurrence of a major climate-cryosphere regime shift (figure 7) linked to the recent rapid winter warming (Nordli *et al* 2014, Isaksen *et al* 2016, López-Moreno *et al* 2016). Previous remote-sensing studies have indicated a strong effect of Arctic winter rain on basal ice formation and snowpack hardening using satellite data (e.g. Grenfell and Putkonen, 2008, Bartsch *et al* 2010, Langlois *et al* 2017) and snowpack simulations (e.g. Vikhamar-Schuler *et al* 2013). However, the very few long-term *in situ* studies in the high Arctic are from Svalbard (Kohler and Aanes 2004, Hansen *et al* 2011, Loe *et al* 2016). By combining these empirical time-series data, we have improved our predictive mechanistic understanding of the environmental conditions causing variation in basal ice in time and space. As expected, basal ice occurrence and thickness increased strongly with the amount of winter rain, particularly so when the accumulated snowfall until the largest rain event was high (figure 5, see also Putkonen and Roe 2003). Accordingly, for a given total snowfall amount, annual snow depths were negatively related to basal ice thickness (figure 4). Since ROS events generally occur over a substantial area (e.g. Rennert *et al* 2009) and are strongly correlated across Svalbard (figure 6(a)), observed basal ice thickness was also strongly correlated across sampling sites (figures 6(b)–(c), S6). This supports previous studies showing that icing events tend to occur across large spatial scales (Bartsch *et al* 2010, Hansen *et al* 2014, Forbes *et al* 2016).

The positive interaction effect of rain and accumulated snowfall on basal ice likely relates to the complex thermodynamic process of latent heat exchange as rain percolates through the snowpack (Woo *et al* 1982, Marsh and Woo 1984, Westermann *et al* 2011). For low amounts of rain falling on top of a deep snowpack, water may fill in the pore space between the snow grains and freeze, or may flow laterally through subsurface layers (Marsh and Woo 1984, Conway and Raymond 1993), thus forming ice layers within the snowpack rather than on the ground surface (supplementary material 7). In contrast, substantial quantities of rainfall during a warm spell will likely percolate through the entire snowpack, as it becomes saturated (Conway and Raymond 1993, Putkonen and Roe 2003, Westermann *et al* 2011). Furthermore, latent heat exchange between rain and snow may increase the cumulative water runoff (Würzer *et al* 2016), thus increasing the formation of basal ice as melted snow and rainwater freezes on the frozen ground.

Winter rain may occur at near-surface temperatures below 0 °C (i.e. 'freezing rain') due to vertical isothermal gradients in the atmosphere with melting layers at higher altitudes and sub-freezing layers towards the ground (Roberts and Stewart 2008). Particularly in coastal regions such as Ny-Ålesund, warmer moist air from the sea may be transported to higher atmospheric layers above land. However, most heavy rain events occur during extreme warm spells coupled with increased wind and air moisture (Hansen *et al* 2014), which boost turbulent fluxes and snowmelt. Therefore, our winter rain variable based on a 1 °C threshold is likely to capture the combined effect of rain and increased temperature on basal ice. The western and southern coastal regions of Spitsbergen generally experience more rainfall (Van Pelt *et al* 2016), and thus heavier basal ice formation, compared to the inner fjord areas of Svalbard. Furthermore, on a more local scale, the positive effect of rainfall amount on basal ice thickness decreased at higher elevations (table 1), because winter precipitation is more likely to fall as snow due to lower ambient temperature at higher altitudes (see also Van Pelt *et al* 2016). Such an effect has also been proposed as a main explanation for why reindeer tend to climb up steep mountain slopes to forage when pastures at lower elevations are covered by ice (Hansen *et al* 2010).

Our models suggest that heavy rainfall that occurs early in winter is less likely to result in basal ice, as little snow has accumulated early in the season. Furthermore, the effect of winter rain on basal ice depends not only on snow cover, but also on other snowpack properties, such as initial liquid water content (Würzer *et al* 2016), linked with variation in air and ground temperatures as well as past icing events. Indeed, increased water run-off and drainage, rather than ice development, would be expected when ground temperatures are close to or above zero and/or air temperatures are not sufficiently low following warm spells. We should therefore expect more complex, non-linear relationships—especially under future winter climate scenarios (Bintanja and Selten 2014, Moore 2016, Bintanja and Andry 2017)—than those explored here.

While recent winters in Svalbard have become increasingly icy (figure 7), this has mainly been evident through a reduction in the frequency of ice-free winters, rather than increased average ice thickness. With continuously warmer and wetter winters, particularly for the early snow season (López-Moreno *et al* 2016, Bintanja and Andry 2017), and increased permafrost temperatures (Etzelmüller *et al* 2011), rapidly warming sites like Svalbard may soon pass a tipping point where extreme winter rainfall actually results in less basal ice. Nevertheless, the increased frequency in ROS events and the coupled increase in basal ice, leading to a recent climate-cryosphere regime shift, are strong indicators of ongoing and near-future changes in high-arctic terrestrial environments, with potentially wide ecological and socio-economic implications.

Acknowledgments

This research was funded by the Research Council of Norway (Centres of Excellence grant 223257; KLIMAFORSK grant 244647; FORINFRA grant 269758; FRIMEDBIO grant 276080) and Svalbard Environmental Protection Fund (grants 13/74 and 16/113). We thank the Institute of Geophysics of the Polish Academy of Sciences for providing weather data from Hornsund. We also want to thank three anonymous referees for providing constructive feedback to the manuscript, the University Centre in Svalbard and the Sverdrup Station (Norwegian Polar Institute) for help

with logistics, and numerous people for digging snow pits.

ORCID iDs

Bart Peeters https://orcid.org/0000-0002-2341-1035
Leif Egil Loe https://orcid.org/0000-0003-4804-2253
Ketil Isaksen https://orcid.org/0000-0003-2356-5330
Vebjørn Veiberg https://orcid.org/0000-0003-1037-5183
Audun Stien https://orcid.org/0000-0001-8046-7337
Jack Kohler https://orcid.org/0000-0003-1963-054X
Jean-Charles Gallet https://orcid.org/0000-0002-6153-1361
Brage Bremset Hansen https://orcid.org/0000-0001-8763-4361

References

Bartsch A, Kumpula T, Forbes B C and Stammler F 2010 Detection of snow surface thawing and refreezing in the Eurasian Arctic with QuikSCAT: implications for reindeer herding *Ecol. Appl.* **20** 2346–58
Benestad R E, Førland E J and Hanssen-Bauer I 2002 Empirically downscaled temperature scenarios for Svalbard *Atmos. Sci. Lett.* **3** 71–93
Bintanja R and Andry O 2017 Towards a rain-dominated Arctic *Nat. Clim. Change* **7** 263–7
Bintanja R and Selten F M 2014 Future increases in Arctic precipitation linked to local evaporation and sea-ice retreat *Nature* **509** 479–82
Bjerke J W 2011 Winter climate change: ice encapsulation at mild subfreezing temperatures kills freeze-tolerant lichens *Environ. Exp. Bot.* **72** 404–8
Bjerke J W, Treharne R, Vikhamar-Schuler D, Karlsen S R, Ravolainen V, Bokhorst S, Phoenix G K, Bochenek Z and Tømmervik H 2017 Understanding the drivers of extensive plant damage in boreal and Arctic ecosystems: insights from field surveys in the aftermath of damage *Sci. Total Environ.* **599** 1965–76
Bjørnstad O N and Falck W 2001 Nonparametric spatial covariance functions: estimation and testing *Environ. Ecol. Stat.* **8** 53–70
Bulygina O N, Groisman P Y, Razuvaev V N and Radionov V F 2010 Snow cover basal ice layer changes over Northern Eurasia since 1966 *Environ. Res. Lett.* **5** 015004
Burnham K P and Anderson D R 2002 *Model Selection and Multimodel Inference: A Practical Information-Theoretic Approach* (New York: Springer)
Christiansen H H, Humlum O and Eckerstorfer M 2013 Central Svalbard 2000–2011 meteorological dynamics and periglacial landscape response *Arctic, Antarct., Alpine Res.* **45** 6–18
Cnaan A, Laird N M and Slasor P 1997 Using the general linear mixed model to analyse unbalanced repeated measures and longitudinal data *Stat. Med.* **16** 2349–80
Conway H and Benedict R 1994 Infiltration of water into snow *Water Resour. Res.* **30** 641–9
Conway H and Raymond C F 1993 Snow stability during rain *J. Glaciol.* **39** 635–42
Coulson S J, Leinaas H P, Ims R A and Søvik G 2000 Experimental manipulation of the winter surface ice layer: the effects on a high Arctic soil microarthropod community *Ecography* **23** 299–306
Eckerstorfer M, Malnes E and Christiansen H H 2017 Freeze/thaw conditions at periglacial landforms in Kapp Linné, Svalbard, investigated using field observations, *in situ*, and radar satellite monitoring *Geomorphology* **293** 433–47
Etzelmüller B, Schuler T V, Isaksen K, Christiansen H H, Farbrot H and Benestad R 2011 Modeling the temperature evolution of Svalbard permafrost during the 20th and 21st century *Cryosphere* **5** 67–79
Forbes B C *et al* 2016 Sea ice, rain-on-snow and tundra reindeer nomadism in Arctic Russia *Biol. Lett.* **12** 20160466
Forchhammer M and Boertmann D 1993 The muskoxen *Ovibos moschatus* in the North and Northeast Greenland—population trends and the influence of abiotic parameters on population-dynamics *Ecography* **16** 299–308
Førland E J, Benestad R, Hanssen-Bauer I, Haugen J E and Skaugen T E 2011 Temperature and precipitation development at Svalbard 1900–2100 *Adv. Meteorol.* **2011** 1–14
Graham R M, Cohen L, Petty A A, Boisvert L N, Rinke A, Hudson S R, Nicolaus M and Granskog M A 2017 Increasing frequency and duration of Arctic winter warming events *Geophys. Res. Lett.* **44** 6974–83
Grenfell T C and Putkonen J 2008 A method for the detection of the severe rain-on-snow event on Banks Island, October 2003, using passive microwave remote sensing *Water Resour. Res.* **44** W03425
Hansen B B, Aanes R, Herfindal I, Kohler J and Sæther B-E 2011 Climate, icing, and wild arctic reindeer: past relationships and future prospects *Ecology* **92** 1917–23
Hansen B B, Aanes R and Sæther B-E 2010 Feeding-crater selection by high-arctic reindeer facing ice-blocked pastures *Can. J. Zoology* **88** 170–7
Hansen B B, Grøtan V, Aanes R, Sæther B-E, Stien A, Fuglei E, Ims R A, Yoccoz N G and Pedersen Å Ø 2013 Climate events synchronize the dynamics of a resident vertebrate community in the high Arctic *Science* **339** 313–5
Hansen B B, Isaksen K, Benestad R E, Kohler J, Pedersen Å Ø, Loe L E, Coulson S J, Larsen J O and Varpe Ø 2014 Warmer and wetter winters: characteristics and implications of an extreme weather event in the high Arctic *Environ. Res. Lett.* **9** 114021
Hock R 1999 A distributed temperature-index ice- and snowmelt model including potential direct solar radiation *J. Glaciol.* **45** 101–11
Isaksen K, Benestad R E, Harris C and Sollid J L 2007 Recent extreme near-surface permafrost temperatures on Svalbard in relation to future climate scenarios *Geophys. Res. Lett.* **34** L17502
Isaksen K, Nordli Ø, Førland E J, Łupikasza E, Eastwood S and Niedźwiedź T 2016 Recent warming on Spitsbergen—influence of atmospheric circulation and sea ice cover *J. Geophys. Res.: Atmos.* **121** 11913–31
Kausrud K L *et al* 2008 Linking climate change to lemming cycles *Nature* **456** 93–7
Kohler J and Aanes R 2004 Effect of winter snow and ground-icing on a Svalbard reindeer population: results of a simple snowpack model *Arctic, Antarct., Alpine Res.* **36** 333–41
Langlois A *et al* 2017 Detection of rain-on-snow (ROS) events and ice layer formation using passive microwave radiometry: a context for Peary caribou habitat in the Canadian Arctic *Remote Sens. Environ.* **189** 84–95
Loe L E *et al* 2016 Behavioral buffering of extreme weather events in a high-Arctic herbivore *Ecosphere* **7** e01374
López-Moreno J I, Boike J, Sanchez-Lorenzo A and Pomeroy J W 2016 Impact of climate warming on snow processes in Ny-Ålesund, a polar maritime site at Svalbard *Glob. Planet. Change* **146** 10–21
Marks D, Kimball J, Tingey D and Link T 1998 The sensitivity of snowmelt processes to climate conditions and forest cover during rain-on-snow: a case study of the 1996 Pacific Northwest flood *Hydrol. Process.* **12** 1569–87
Marsh P and Woo M-K 1984 Wetting front advance and freezing of meltwater within a snow cover: 1. Observations in the Canadian Arctic *Water Resour. Res.* **20** 1853–64

Miller F L and Gunn A 2003 Catastrophic die-off of Peary caribou on the western queen Elizabeth Islands, Canadian high Arctic *Arctic* **56** 381–90

Milner J M, Varpe Ø, Van der Wal R and Hansen B B 2016 Experimental icing affects growth, mortality, and flowering in a high Arctic dwarf shrub *Ecol. Evol.* **6** 2139–48

Moore G W K 2016 The December 2015 North Pole warming event and the increasing occurrence of such events *Sci. Rep.* **6** 39084

Nakagawa S and Schielzeth H 2013 A general and simple method for obtaining R^2 from generalized linear mixed-effects models *Methods Ecol. Evol.* **4** 133–42

Nordli Ø, Przybylak R, Ogilvie A E J and Isaksen K 2014 Long-term temperature trends and variability on Spitsbergen: the extended Svalbard Airport temperature series, 1898-2012 *Polar Res.* **33** 21349

Overland J E, Percival D B and Mofjeld H O 2006 Regime shifts and red noise in the North Pacific *Deep Sea Res.* I **53** 582–8

Parker G A, Thomas D C, Broughton E and Gray D R 1975 Crashes of muskox and Peary caribou populations in 1973–74 in the Parry islands, Arctic Canada *Can. Wildlife Serv. Prog. Notes* **56** 1–10

Preece C, Callaghan T V and Phoenix G K 2012 Impacts of winter icing events on the growth, phenology and physiology of sub-arctic dwarf shrubs *Physiol. Plantarum* **146** 460–72

Putkonen J and Roe G 2003 Rain-on-snow events impact soil temperatures and affect ungulate survival *Geophys. Res. Lett.* **30** 1188–92

Rennert K J, Roe G, Putkonen J and Bitz C M 2009 Soil thermal and ecological impacts of rain on snow events in the circumpolar Arctic *J. Clim.* **22** 2302–15

Riseth J Å, Tømmervik H and Bjerke J W 2016 175 years of adaptation: North Scandinavian Sámi reindeer herding between government policies and winter climate variability (1835–2010) *J. Forest Econ.* **24** 186–204

Roberts E and Stewart R E 2008 On the occurrence of freezing rain and ice pellets over the eastern Canadian Arctic *Atmos. Res.* **89** 93–109

Serreze M C, Barrett A P, Stroeve J C, Kindig D N and Holland M M 2009 The emergence of surface-based Arctic amplification *Cryosphere* **3** 11–9

Stien A *et al* 2012 Congruent responses to weather variability in high arctic herbivores *Biol. Lett.* **8** 1002–5

Van Pelt W J J, Kohler J, Liston G E, Hagen J O, Luks B, Reijmer C H and Pohjola V A 2016 Multidecadal climate and seasonal snow conditions in Svalbard *J. Geophys. Res.: Earth Surf.* **121** 2100–17

Vikhamar-Schuler D, Hanssen-Bauer I, Schuler T V, Mathiesen S D and Lehning M 2013 Use of a multilayer snow model to assess grazing conditions for reindeer *Ann. Glaciol.* **54** 214–26

Vikhamar-Schuler D, Isaksen K, Haugen J E, Tømmervik H, Luks B, Schuler T V and Bjerke J W 2016 Changes in winter warming events in the Nordic Arctic region *J. Clim.* **29** 6223–44

Westermann S, Boike J, Langer M, Schuler T V and Etzelmüller B 2011 Modeling the impact of wintertime rain events on the thermal regime of permafrost *Cryosphere* **5** 945–59

Woo M-K, Heron R and Marsh P 1982 Basal Ice in High Arctic Snowpacks *Arctic, Alpine Res.* **14** 251–60

Würzer S, Jonas T, Wever N and Lehning M 2016 Influence of initial snowpack properties on runoff formation during rain-on-snow events *J. Hydrometeorol.* **17** 1801–15

Zhang X, He J, Zhang J, Polyakov I, Gerdes R, Inoue J and Wu P 2012 Enhanced poleward moisture transport and amplified northern high-latitude wetting trend *Nat. Clim. Change* **3** 47–51